JACS
JOURNAL OF THE AMERICAN CHEMICAL SOCIETY
Communication
pubs.acs.org/JACS

High-Temperature Ferrimagnetism Driven by Lattice Distortion in Double Perovskite Ca_2FeOsO_6

Hai L. Feng,*[,†,‡] Masao Arai,[§] Yoshitaka Matsushita,[∥] Yoshihiro Tsujimoto,[⊥] Yanfeng Guo,[†,▽] Clastin I. Sathish,[†,‡] Xia Wang,[†] Ya-Hua Yuan,[†,‡] Masahiko Tanaka,[#] and Kazunari Yamaura*[,†,‡]

[†]Superconducting Properties Unit, National Institute for Materials Science, 1-1 Namiki, Tsukuba, Ibaraki 305-0044, Japan
[‡]Graduate School of Chemical Sciences and Engineering, Hokkaido University, North 10 West 8, Kita-ku, Sapporo, Hokkaido 060-0810, Japan
[§]Computational Materials Science Center, National Institute for Materials Science, 1-1 Namiki, Tsukuba, Ibaraki 305-0044, Japan
[∥]Materials Analysis Station, National Institute for Materials Science, 1-2-1 Sengen, Tsukuba, Ibaraki 305-0047, Japan
[⊥]Materials Processing Unit, National Institute for Materials Science, 1-2-1 Sengen, Tsukuba, Ibaraki 305-0047, Japan
[#]Synchrotron X-ray Station at SPring-8, National Institute for Materials Science, Kohto 1-1-1, Sayo-cho, Hyogo 679-5148, Japan

Supporting Information

ABSTRACT: 5d and 3d hybrid solid-state oxide Ca_2FeOsO_6 crystallizes into an ordered double-perovskite structure with a space group of $P2_1/n$ with high-pressures and temperatures. Ca_2FeOsO_6 presents a long-range ferrimagnetic transition at a temperature of ∼320 K (T_c) and is not a band insulator, but is electrically insulating like the recently discovered Sr_2CrOsO_6 (T_c ∼725 K). The electronic stat of Ca_2FeOsO_6 is adjacent to a half-metallic state as well as that of Sr_2CrOsO_6. In addition, the high-T_c ferrimagnetism was driven by lattice distortion, which was observed for the first time among double-perovskite oxides and represents complex interplays between spins and orbitals. Unlike conventional ferrite and garnet, the interplays likely play a pivotal role of the ferrimagnetism. A new class of 5d−3d hybrid ferrimagnetic insulators with high-T_c is established to develop practically and scientifically useful spintronic materials.

Solid-state perovskite oxides, with the general structure ABO_3, with unpaired d-electrons show scientifically and practically useful electromagnetic properties such as ferromagnetism, multiferroicity, and colossal magnetoresistance, depending on the combinations of A (alkali metal, alkali earth metal, rare earth metal, or solution of those) and B (transition metal). Most of the useful properties appear when B is a 3d element, probably because unpaired 3d electrons strongly correlate with each other or with oxygen 2p electrons in the perovskite lattice.[1] For example, the on-site Coulomb interaction U, which roughly outlines the degree of electronic correlations is in the range of 2−10 eV for 3d perovskite oxides,[2,3] while U of 5d perovskite oxides is usually <∼1 eV.[2,3]

Recently, 5d(4d)−3d hybrid solid-state oxides have attracted great attention due to the half-metallic (HM) nature found in double perovskite oxides Sr_2FeMoO_6[4−6] and Sr_2FeReO_6,[7−9] which exhibit spin-polarized transitions at temperatures greater than 400 K. The double perovskite oxide is usually denoted as $A_2BB'O_6$, where B and B′ atoms are ordered, doubling the unit cell of ABO_3. In the HM state, 3d−t_{2g} and 5d(4d)−t_{2g} electrons in the B and B′ sites, respectively, play a pivotal role in the highly spin-polarized conduction, which was argued to result from a generalized double exchange mechanism.[10,11] The high temperatures imply possible developments of novel spintronic applications, which may work without cooling. Furthermore, additional double perovskite oxides have been suggested to be HM at room temperature.[7,12−23] Therefore, prospects for spintronics applications are very high and enormous efforts have been made not only to develop HM properties, but also to explore novel 5d(4d)−3d hybrid properties.

The double perovskite oxide Sr_2CrOsO_6, which was synthesized in 2007, showed a ferrimagnetic (FIM) transition at T_c of ∼725 K,[24] the highest reported T_c of the perovskite and double perovskite oxides.[16] However, the generalized double exchange mechanism was unable to account for the 725 K transition because Sr_2CrOsO_6 is a multiorbital Mott insulator and the FIM state is thus distinguishable from the HM state.[25] The high-T_c FIM transition was novel; therefore, an additional 5d−3d hybrid high-T_c FIM oxide was highly desired to elucidate the mechanism of the high-T_c transition.

Here we report a novel double perovskite oxide, Ca_2FeOsO_6, synthesized using a high-temperature and pressure. It crystallizes into a monoclinic double perovskite structure like many double perovskite oxides. Notably, it shows an FIM transition at a T_c of 320 K. It is not a band insulator, but is highly insulating electrically. Thus, the explanation for the high-T_c FIM transition of Ca_2FeOsO_6 is likely similar to that of Sr_2CrOsO_6.

Polycrystalline Ca_2FeOsO_6 was synthesized by solid-state reaction under high-pressure, and the final product was characterized using synchrotron X-ray diffraction (SXRD; see Supporting Information for details). The SXRD study determined the crystal structure of Ca_2FeOsO_6 to be monoclinic with a space group of $P2_1/n$, as was reported for many B-site ordered double perovskites.[26,27] The refined SXRD patterns are shown in Figure 1. Generally in a double

Received: November 17, 2013
Published: February 17, 2014

   dx.doi.org/10.1021/ja411713q | J. Am. Chem. Soc. 2014, 136, 3326−3329

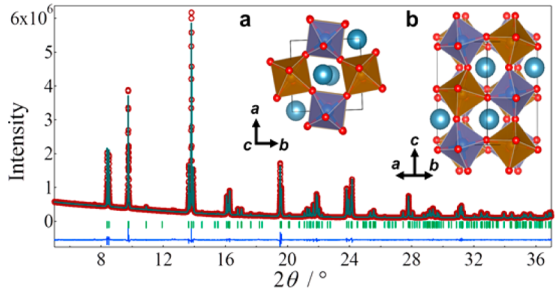

Figure 1. Rietveld refined SXRD profiles of Ca_2FeOsO_6. Inset (a) is a crystallographic view along the [001] direction and (b) along the [110] direction. The blue and brown octahedral represent FeO_6 and OsO_6, respectively. The solid spheres represent Ca.

perovskite structure, the degree of the B-site order depends on synthetic conditions ranging from 100% ordered (an ordered rock-salt type) to 0% ordered (a disordered type). Thus, during the refinements, Fe and Os ions were randomly mixed at the same crystallographic site in a 1:1 molar ratio. However, we were unable to reach a reasonable structure solution using these conditions. Alternatively, Fe and Os could be assumed to occupy independent sites. In subsequent refinements, the displacement parameters were temporally fixed at 0.5 $Å^2$, while the occupancies were fixed. Finally, the analysis indicated that Fe and Os atoms were ordered approximately 90% in the B-site. The small imperfection may be related to the proximity of the ionic radii of Fe^{3+} (0.645 Å) and Os^{5+} (0.575 Å).[28,29] The cell parameters of Ca_2FeOsO_6 were a = 5.3931(6) Å, b = 5.5084(3) Å, c = 7.6790(3) Å, and β = 89.0211(49)°. The reliable indexes were R_p = 1.81% and R_{wp} = 2.95%.[30] Details of the analysis are summarized in Tables S1 and S2.

The average bond length of Os^{5+}−O was ∼1.956 Å, comparable to that of Os^{5+}−O in other perovskite oxides (1.946 Å for $NaOsO_3$[31] and 1.960 Å for La_2NaOsO_6).[32] The bond valence sum, calculated from the bond distances,[33,34] was 3.00 for Fe and 4.74 for Os, indicating 3+ and 5+ valence states of the atoms, respectively.[33] Bond valence parameters r_{Fe-O} = 1.751, r_{Os-O} = 1.868, and B = 0.37 were used in the estimation.[34]

The average bond length of Fe^{3+}−O (2.005 Å) was comparable or slightly larger than that of Ca_2FeMoO_6 (2.026 Å) and Sr_2FeOsO_6 (1.938 Å); hence, it is reasonable to conclude that Fe^{3+} of Ca_2FeOsO_6 is in the high-spin state as well as Fe^{3+} of Ca_2FeMoO_6[35] and Sr_2FeOsO_6.[36] Note that a high-spin to low-spin state transition via intermediate-spin state of Fe^{3+} in octahedral environment usually occurs at extremely high-pressure conditions far beyond 6 GPa.[37,38] Comprehensive high-pressure studies of Fe oxides also imply the high-spin state for Fe^{3+} of Ca_2FeOsO_6.[37,38]

The crystal structure of Ca_2FeOsO_6 is shown in Figure 1, based on the experimental solution, showing that Fe and Os ions alternate to occupy the octahedra like a checker board. Bond angles of the interoctahedral Fe−O−Os are 151° and 154°, which are far from 180°, indicating significant buckling of the octahedral connection. Insets a and b show alternate rotations of the octahedra along and perpendicular to the c axis, respectively. The Glazer's notation is $a^-a^-b^+$, where the superscripts indicate that neighbor octahedra rotated in the same ($^+$) and opposite ($^-$) direction.[39] The degree of distortion is clearly more enhanced than that of Sr_2FeOsO_6, where the interoctahedral Fe−O−Os are 180° and 165°.[36]

Isothermal magnetizations of Ca_2FeOsO_6 at 2 and 300 K are compared with those of Sr_2FeOsO_6 in Figure 2. The

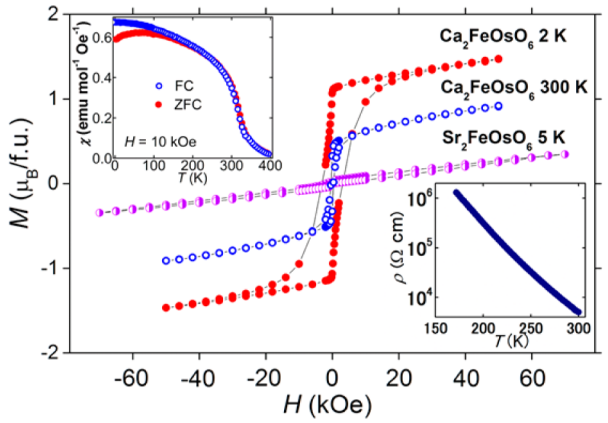

Figure 2. Isothermal magnetizations of Ca_2FeOsO_6 and Sr_2FeOsO_6.[36] Upper and lower insets show temperature dependent magnetic susceptibility and electrical resistivity of polycrystalline Ca_2FeOsO_6, respectively.

spontaneous magnetization of Ca_2FeOsO_6 was 1.2 μ_B/f.u. at 2 K (0.5 μ_B/f.u. at 300 K). This was in large contrast to the near zero magnetization of isoelectronic Sr_2FeOsO_6.[36] The observed magnetization was, however, much lower than the theoretical sum of the spin only moment 8.0 μ_B/f.u. of Fe^{3+} (t_{2g}^3 e_g^2) and Os^{5+} (t_{2g}^3). It was closer to the difference of each spin only moment (2.0 μ_B/f.u). Temperature dependent magnetic susceptibility in an applied field of 10 kOe is shown in the upper inset of Figure 2. A remarkable increase was observed approximately 320 K, indicating the occurrence of a long-range magnetic order. Specific heat measurements revealed that it is a bulk transition (Figure S1a). The measurements therefore suggest that an FIM order is established at 320 K with cooling (Figure S2).

A small disagreement between the observed moment (1.2 μ_B/f.u.) and the theoretical FIM spin-only moment (2.0 μ_B/f.u.) was partly due to the imperfect order of Fe/Os atoms. The disorder should decrease the magnetic moment as follows: $M = M_{exp} \times (1-2AS)$, where M_{exp} is the expected moment and AS is the degree of disorder between Fe and Os atoms.[40−42] In Ca_2FeOsO_6, M_{exp} was 2 μ_B/f.u. and AS was 0.1 (10% disorder), resulting in 1.6 μB/f.u., approaching the observed moment of 1.2 μ_B/f.u. In addition, rather stronger hybridization between 5d and oxygen 2p orbitals may reduce the local magnetic moments to some extent, accounting in part for the overestimation of the magnetic moment.

The lower inset of Figure 2 shows the temperature dependent electrical resistivity (ρ) of Ca_2FeOsO_6. At room temperature, the ρ was approximately 5 kΩ·cm and continued to increase upon cooling beyond the instrumental limit. The seemingly semiconducting temperature dependence was well characterized by the Arrhenius model; the activation energy was estimated to be 1.2 eV within the available temperature range (Figure S3). To further confirm the bulk semiconducting behavior, the electronic structure of Ca_2FeOsO_6 was investigated by means of first-principle calculations as shown in Figure S4. The result clearly indicated that Ca_2FeOsO_6 is metallic in nature, contradicting the observation in the ρ vs T measurement. Alternatively, the spin-polarized calculation resulted in a stable solution with a substantial charge gap as

dx.doi.org/10.1021/ja411713q | J. Am. Chem. Soc. 2014, 136, 3326−3329

shown in Figure S5. Therefore, an antiparallel arrangement of the Os and Fe moments (the up-spin state of Os and downspin state of Fe are preferably occupied) can be expected as the true ground state of Ca_2FeOsO_6. The Sommerfeld coefficient was nearly zero in the specific-heat measurements (Figure S1b), supporting the notion of a full charge gap. The theoretical study suggested that the spin-polarization is essential to account for the observed FIM and semiconducting properties.

On the basis of the results above, the most probable magnetic state is proposed in Figure 3a and compared with the

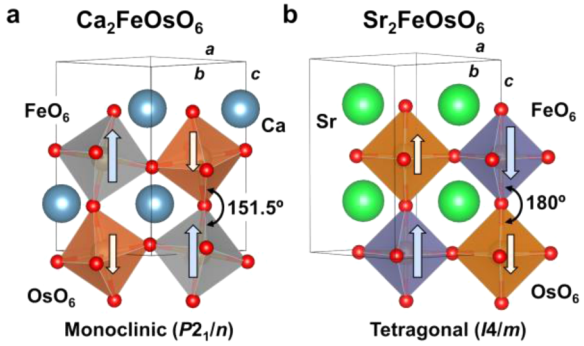

Figure 3. Proposed magnetic ordered state of (a) Ca_2FeOsO_6 and (b) comparison with the AF1 state of Sr_2FeOsO_6 (sketched from refs 25 and 36). Note that arrow denotes either up-spin or down-spin.

antiferromagnetic (AF) model proposed for Sr_2FeOsO_6 (the AF1 phase)[25,36] seen in Figure 3b. The nearest-neighbor spin interaction is mediated by superexchange interactions via Fe^{3+}−O−Os^{5+} in both compounds.[43] Regarding Sr_2FeOsO_6, it was argued that the superexchange interaction along the *c* axis was ferromagnetic (FM) because of the nature of the 180° d^3−d^5 bond. An artificial superlattice of $LaFeO_3/LaCrO_3$ consisting of a similar 180° d^3−d^5 bond was indeed FM below 375 K.[44] Meanwhile, the Fe−O−Os bond in the *ab* plane significantly bends to 165°, leading AF order in the *ab* plane.[43] Very recently, the proposed model of Sr_2FeOsO_6 was confirmed by neutron diffraction.[25] In contrast, Ca_2FeOsO_6 has Fe^{3+}−O−Os^{5+} bonds at 151−154° along and perpendicular to the *c* axis, respectively. Because the d^3−d^5 superexchange interaction varies from FM to AF in a range of 125−150°,[43] the proposed FIM model does not violate the superexchange model.[43]

The high-T_c FIM state of Ca_2FeOsO_6 was adapted from the AF state of Sr_2FeOsO_6 through a lattice distortion. Thus, the AF to FIM transition driven by lattice distortion was observed for the first time among double perovskite oxides, and is perhaps one of the few examples in all known solid-state oxides. Therefore, Ca_2FeOsO_6 represents not only a practically useful form of magnetism, but also a scientifically exotic state.

In conclusion, the novel double perovskite oxide Ca_2FeOsO_6 was synthesized under a pressure of 6 GPa, and it crystallized into a monoclinic structure with a space group of $P2_1/n$. The magnetic and specific-heat measurements characterized the FIM transition at T_c of 320 K. The ρ measurement revealed the electrically insulating state with an activation energy of 1.2 eV, although Ca_2FeOsO_6 is not a band insulator. The theoretical consideration of the electronic structure draws the highly spin-polarized Fe-3d and Os-5d FIM picture, which is near the HM state [see Figure S5, in which the magnetic moments in atomic spheres are evaluated as 4.02 μ_B for Fe and −1.46 μ_B for Os without spin−orbit (SO) interaction and 4.02 μ_B for Fe and −1.34 μ_B for Os with SO interaction]. Although the SO interaction seems to be insignificant, complex interplays between spins and orbitals likely play an important role in establishing the FIM state of Ca_2FeOsO_6, unlike what was found in conventional FIM materials such as ferrite and garnet.[45] This was supported by the drastic impact of the lattice distortion on the magnetism, in addition to the competing spin structures recently discovered in the isoelectronic Sr_2FeOsO_6.[25]

Ca_2FeOsO_6 and Sr_2CrOsO_6 establish a new class of high-T_c 5d−3d hybrid FIM insulators, which is adjacent to the HM state and hence can be useful for scientific and practical applications in spintronics. The origin of the novel FIM transition with the remarkably higher T_c of 320 K for Ca_2FeOsO_6 and 725 K for Sr_2CrOsO_6 remains to be elucidated and further studies including carrier doping to the novel FIM state are in progress as well as neutron diffraction study.

■ ASSOCIATED CONTENT

Supporting Information

Includes synthesis and characterization of the compound. The refined atom coordination, selected bond lengths and angles. Specific heat, inverse magnetic susceptibility, and electrical resistivity analysis. The total density of states of Ca_2FeOsO_6 based on the GGA, GGA+SOC, and GGA+U calculations, respectively. This material is available free of charge via the Internet at http://pubs.acs.org.

■ AUTHOR INFORMATION

Corresponding Authors

Hai.FENG_NIMS@hotmail.com
YAMAURA.Kazunari@nims.go.jp

Present Address

[V]Condensed Matter Physics, Clarendon Laboratory, University of Oxford, Parks Road, Oxford OX1 3PU, United Kingdom (Y.F.G.).

Notes

The authors declare no competing financial interest.

■ ACKNOWLEDGMENTS

This research was supported in part by the World Premier International Research Center of the Ministry of Education, Culture, Sports, Science and Technology (MEXT) of Japan, by the Japan Society for the Promotion of Science (JSPS) through a Grant-in-Aid for Scientific Research (25289233), and by the Funding Program for World-Leading Innovative R&D on Science and Technology (FIRST Program), Japan. The authors thank the staff of BL15XU, the National Institute for Materials Science (NIMS), and SPring-8 for their help with the use of the beamline. We performed the SXRD measurements with the approval of the NIMS beamline station (Proposal No. 2012B4506, 2013A4504, 2013B4503).

■ REFERENCES

(1) Imada, M.; Fujimori, A.; Tokura, Y. *Rev. Mod. Phys.* **1998**, *70*, 1039.
(2) Haskel, D.; Fabbris, G.; Zhernenkov, M.; Kong, P. P.; Jin, C. Q.; Cao, G.; van Veenendaal, M. *Phys. Rev. Lett.* **2012**, *109*, 027204.
(3) Laguna-Marco, M. A.; Haskel, D.; Souza-Neto, N.; Lang, J. C.; Krishnamurthy, V. V.; Chikara, S.; Cao, G.; van Veenendaal, M. *Phys. Rev. Lett.* **2010**, *105*, 216407.
(4) Kobayashi, K. L.; Kimura, T.; Sawada, H.; Terakura, K.; Tokura, Y. *Nature* **1998**, *395*, 677.
(5) Sarma, D. D.; Mahadevan, P.; Saha-Dasgupta, T.; Ray, S.; Kumar, A. *Phys. Rev. Lett.* **2000**, *85*, 2549.

(6) Tomioka, Y.; Okuda, T.; Okimoto, Y.; Kumai, R.; Kobayashi, K. I.; Tokura, Y. *Phys. Rev. B* **2000**, *61*, 422.
(7) Jeng, H. T.; Guo, G. Y. *Phys. Rev. B* **2003**, *67*, 094438.
(8) Kobayashi, K. I.; Kimura, T.; Tomioka, Y.; Sawada, H.; Terakura, K.; Tokura, Y. *Phys. Rev. B* **1999**, *59*, 11159.
(9) Solovyev, I. V. *Phys. Rev. B* **2002**, *65*, 144446.
(10) Kanamori, J.; Terakura, K. *J. Phys. Soc. Jpn.* **2001**, *70*, 1433.
(11) Erten, O.; Meetei, O. N.; Mukherjee, A.; Randeria, M.; Trivedi, N.; Woodward, P. *Phys. Rev. Lett.* **2011**, *107*, 257201.
(12) Chmaissem, O.; Dabrowski, B.; Kolesnik, S.; Short, S.; Jorgensen, J. D. *Phys. Rev. B* **2005**, *71*, 174421.
(13) Popov, G.; Greenblatt, M.; Croft, M. *Phys. Rev. B* **2003**, *67*, 024406.
(14) Arulraj, A.; Ramesha, K.; Gopalakrishnan, J.; Rao, C. N. R. *J. Solid State Chem.* **2000**, *155*, 233.
(15) Wu, H. *Phys. Rev. B* **2001**, *64*, 125126.
(16) Serrate, D.; De Teresa, J. M.; Ibarra, M. R. *J. Phys.: Condens. Matter* **2007**, *19*, 023201.
(17) Vaitheeswaran, G.; Kanchana, V.; Delin, A. *Appl. Phys. Lett.* **2005**, *86*, 032513.
(18) Kato, H.; Okuda, T.; Okimoto, Y.; Tomioka, Y.; Takenoya, Y.; Ohkubo, A.; Kawasaki, M.; Tokura, Y. *App. Phys. Lett.* **2002**, *81*, 328.
(19) Philipp, J. B.; Majewski, P.; Alff, L.; Erb, A.; Gross, R.; Graf, T.; Brandt, M. S.; Simon, J.; Walther, T.; Mader, W.; Topwal, D.; Sarma, D. D. *Phys. Rev. B* **2003**, *68*, 144431.
(20) Philipp, J. B.; Reisinger, D.; Schonecke, M.; Marx, A.; Erb, A.; Alff, L.; Gross, R.; Klein, J. *Appl. Phys. Lett.* **2001**, *79*, 3654.
(21) De Teresa, J. M.; Serrate, D.; Blasco, J.; Ibarra, M. R.; Morellon, L. *Phys. Rev. B* **2004**, *69*, 144401.
(22) Kato, H.; Okuda, T.; Okimoto, Y.; Tomioka, Y.; Oikawa, K.; Kamiyama, T.; Tokura, Y. *Phys. Rev. B* **2002**, *65*, 144404.
(23) Prellier, W.; Smolyaninova, V.; Biswas, A.; Galley, C.; Greene, R. L.; Ramesha, K.; Gopalakrishnan, J. *J. Phys.: Condens. Matter* **2000**, *12*, 965.
(24) Krockenberger, Y.; Mogare, K.; Reehuis, M.; Tovar, M.; Jansen, M.; Vaitheeswaran, G.; Kanchana, V.; Bultmark, F.; Delin, A.; Wilhelm, F.; Rogalev, A.; Winkler, A.; Alff, L. *Phys. Rev. B* **2007**, *75*, 020404.
(25) Meetei, O. N.; Erten, O.; Randeria, M.; Trivedi, N.; Woodward, P. *Phys. Rev. Lett.* **2013**, *110*, 087203.
(26) Abakumov, A. M.; Shpanchenko, R. V.; Antipov, E. V.; Lebedev, O. I.; VanTendeloo, G. *J. Solid State Chem.* **1997**, *131*, 305.
(27) Battle, P. D.; Jones, C. W.; Studer, F. *J. Solid State Chem.* **1991**, *90*, 302.
(28) Anderson, M. T.; Greenwood, K. B.; Taylor, G. A.; Poeppelmeier, K. R. *Prog. Solid State Chem.* **1993**, *22*, 197.
(29) Shannon, R. D. *Acta Crystallogr., A* **1976**, *32*, 751.
(30) Momma, K.; Izumi, F. *J. Appl. Crystallogr.* **2008**, *41*, 653.
(31) Shi, Y. G.; Guo, Y. F.; Yu, S.; Arai, M.; Belik, A. A.; Sato, A.; Yamaura, K.; Takayama-Muromachi, E.; Tian, H. F.; Yang, H. X.; Li, J. Q.; Varga, T.; Mitchell, J. F.; Okamoto, S. *Phys. Rev. B* **2009**, *80*, 161104.
(32) Gemmill, W. R.; Smith, M. D.; Prozorov, R.; Loye, H. C. Z. *Inorg. Chem.* **2005**, *44*, 2639.
(33) Brese, N. E.; Okeeffe, M. *Acta Crystallogr., B* **1991**, *47*, 192.
(34) Brown, I. D.; Altermatt, D. *Acta Crystallogr., B* **1985**, *41*, 244.
(35) Alonso, J. A.; Casais, M. T.; Martinez-Lope, M. J.; Martinez, J. L.; Velasco, P.; Munoz, A.; Fernandez-Diaz, M. T. *Chem. Mater.* **2000**, *12*, 161.
(36) Paul, A. K.; Jansen, M.; Yan, B. H.; Felser, C.; Reehuis, M.; Abdala, P. M. *Inorg. Chem.* **2013**, *52*, 6713.
(37) Ju, S.; Cai, T. Y.; Lu, H. S.; Gong, C. D. *J. Am. Chem. Soc.* **2012**, *134*, 13780.
(38) Ding, Y.; Haskel, D.; Ovchinnikov, S. G.; Tseng, Y.-C.; Orlov, Y. S.; Lang, J. C.; Mao, H.-k. *Phys. Rev. Lett.* **2008**, *100*, 045508.
(39) Glazer, A. M. *Acta Crystallogr., B* **1972**, *28*, 3384.
(40) Serrate, D.; De Teresa, J. M.; Ibarra, M. R. *J. Phys.: Condens. Matter* **2007**, *19*, 023201.
(41) Alonso, J. L.; Fernandez, L. A.; Guinea, F.; Lesmes, F.; Martin-Mayor, V. *Phys. Rev. B* **2003**, *67*, 214423.
(42) Michalik, J. M.; De Teresa, J. M.; Ritter, C.; Blasco, J.; Serrate, D.; Ibarra, M. R.; Kapusta, C.; Freudenberger, J.; Kozlova, N. *Europhys. Lett.* **2007**, *78*, 17006.
(43) Goodenough, J. B. *Magnetism and the Chemical Bond*; Interscience: New York, 1963.
(44) Ueda, K.; Tabata, H.; Kawai, T. *Science* **1998**, *280*, 1064.
(45) Spaldin, N. A. *Magnetic Materials: Fundamentals and Applications*, 2nd ed.; Cambridge: Cambridge University Press, 2010; pp 113−129.